Article

pubs.acs.org/Biomac

# Effect of Heparin on Protein Aggregation: Inhibition versus Promotion

Yisheng Xu,[†] Daniel Seeman,[†] Yunfeng Yan,[†] Lianhong Sun,[‡] Jared Post,[†] and Paul L. Dubin*[,†]

[‡]School of Life Sciences, University of Science and Technology of China, Hefei, Anhui, 230027, People's Republic of China

[†]Department of Chemistry, University of Massachusetts, 710 North Pleasant Street, Amherst, Massachusetts 01003

Supporting Information

**ABSTRACT:** The effect of heparin on both native and denatured protein aggregation was investigated by turbidimetry and dynamic light scattering (DLS). Turbidimetric data show that heparin is capable of inhibiting and reversing the native aggregation of bovine serum albumin (BSA), $\beta$-lactoglobulin (BLG), and Zn−insulin at a pH near pI and at low ionic strength $I$; however, the results vary with regard to the range of pH, $I$, and protein−heparin stoichiometry required to achieve these effects. The kinetics of this process were studied to determine the mechanism by which interaction with heparin could result in inhibition or reversal of native protein aggregates. For each protein, the binding of heparin to distinctive intermediate aggregates formed at different times in the aggregation process dictates the outcome of complexation. This differential binding was explained by changes in the affinity of a given protein for heparin, partly due to the effects of protein charge anisotropy as visualized by electrostatic modeling. The heparin effect can be further extended to include inhibition of denaturing protein aggregation, as seen from the kinetics of BLG aggregation under conditions of thermally induced unfolding with and without heparin.

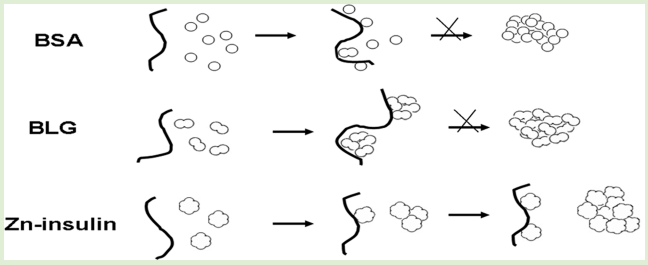


## INTRODUCTION

Heparin has been shown to inhibit protein aggregation both in vivo and in vitro, but there are also reports of the opposite effect. This is because heparin−protein complexes differ in many ways from the species formed by interaction of proteins with a variety of low MW aggregation inhibitors. The various mechanisms proposed in those cases are largely irrelevant to inhibition by polyelectrolytes such as heparin with regard to the conditions for complexation and the properties of the complexes. As a result, heparin may enter into the aggregation pathway in ways that differ from other aggregation inhibitors. An examination of the way in which the effect of heparin depends on aggregation mechanism could help resolve the contradictory literature.

The undesirable consequences of protein aggregation in many areas, for example, protein crystallography,[1] bioprocessing,[2] and pharmacology[3−8] have led to investigation of many antiaggregation agents. Unique among these is heparin whose effects on protein aggregation have been studied for many protein systems in vivo and in vitro, the latter encompassing a wide range of solution conditions. Heparin is able to reverse Zn−insulin aggregation;[9] can decrease temperature-induced aggregation of recombinant human keratinocyte growth factor (rhKGF);[10] and acts as a refolding agent ("artificial chaperone") for creatine kinase.[11] Effects observed in vivo, reducing the induction of inflammation-associated (AA) amyloid,[12] inhibiting the assembly of fibrillin-1 into microfibrillar network in cultures of skin fibroblasts,[13] and complexing inactive agrin before it can induce aggregation of acetylcholine receptors.[14] These findings may have stimulated the use of heparin as a pharmaceutical additive in protein stabilization or aggregation inhibition.[15]

On the contrary, heparin can also promote irreversible protein association. Studies in vitro show that heparin causes instant aggregation of denatured and native lysozyme[16] and can promote the aggregation of recombinant human prion protein.[17] The molecular basis of both effects could be the unique charge sequence arrangements of heparin, which enables it to "promiscuously" complex many proteins thereby possibly reducing aggregation via intercomplex repulsion. Studies of the role of heparinoids in amyloidogenesis have produced less benign results. Heparinoids or other GAGs have been found in almost all amyloid deposits investigated thus far. For this reason, they are thought to be deposited during the course of amyloid fibrilogenesis,[18] thus, playing a direct role in many human diseases,[19−22] although the mechanisms of stimulation of amyloid fibrils by glycoaminoglycans are still unclear.

To explain these apparent contradictions, it is necessary to consider that the formation of soluble complexes between native proteins and heparin[23−27] is only one of several effects observed for polyelectrolyte−protein complexes. These effects

Received: March 5, 2012
Revised: April 5, 2012
Published: April 12, 2012

ACS Publications © 2012 American Chemical Society



dx.doi.org/10.1021/bm3003539 | Biomacromolecules 2012, 13, 1642−1651

include also (1) binding of heparin to soluble aggregates of native or unfolded proteins, (2) the formation of coacervates (liquid−liquid phase separation) from such aggregates, and (3) formation of protein−heparin precipitate (either by transition from coacervate or by flocculation). Only the binding of heparin to native proteins or to soluble aggregates can be considered aggregation inhibition, but the last two can lead to changes in turbidity, complicating interpretation of typical observations. These processes are electrostatically modulated in different ways. Protein−PE interactions in general diminish with ionic strength, $I$, and increase with PE linear charge density and opposing protein charge (in particular, the charge of the protein domain to which PE binds).[28] pH, controlling the last parameter, influences not only binding affinity, but also complex net charge (which in turn controls complex solubility).[28,29] Thus, the final result is that turbidimetry, the usual probe of protein aggregation, becomes highly sensitive to solution conditions and stoichiometry,[30] one way in which reports about heparin's role in aggregation can appear to contradict each other.

The antiaggregative properties of the polyelectrolyte heparin result from its ability to complex the native states of proteins and so compete with self-aggregation.[9,31] The point at which heparin enters the aggregation process is reflected in the terms "inhibition", "suppression", and "reversal", sometimes used synonymously in the protein aggregation literature. "Inhibition" is best used to describe a preaggregation effect, which diverts proteins from the aggregation pathway; in the case of heparin, this involves decreasing or eliminating interactions of proteins that are heparin-bound. "Suppression" on the other hand should refer to the reduction of the protein aggregation rate; in the case of heparin binding, this occurs by reduction in the concentration of free protein. "Reversal" suggests resolubilization of aggregates; in the case of heparin, this arises from the ability of heparin chains to take aggregates apart. The different meanings of these three words indicate that aggregation can proceed through multiple intermediates, different agents interacting with the aggregate itself or its various precursors.

Because heparin can interact with different aggregation precursors and intermediates, elucidation of the effect of heparin requires an understanding of the molecular mechanism of protein aggregation. For native state aggregation, self-association of folded proteins is mediated by electrostatic effects. While the diminution of electrostatic repulsion at pI is relevant, electrostatic attraction at pI, due to charge anisotropy can drive "isoelectric precipitation", as demonstrated by increased solubility with added salt, and aggregation maxima near but not at the pI. The more frequently studied case of partially unfolded proteins[32−34] involves fibrils that are typically characterized by the stacking of $\beta$-sheet structures. Such unfolding aggregation can be induced by heat,[35] extremes of pH,[36] cosolvents, and agitation,[37] with many of these processes involving the exposure of hydrophobic surfaces. For both native and unfolded states, the mechanisms of protein aggregation may include (1) simple growth, in which proteins oligomerize (including dimer, trimer, etc.) in a manner independent of the size of these oligomers,[38] (2) monomer−cluster aggregation or "growth", the addition of individual proteins to preformed protein aggregate,[38−40] (3) cluster−cluster aggregation, in which aggregates of any size can combine, with no sequential addition of monomer units,[39] and (4) nucleation controlled aggregation in which sequential monomer addition takes place only after the cooperative formation of a cluster (nucleus).[38] The exact way in which inhibitors of protein aggregation affect one or more of these processes is often unknown. Our objective here is to investigate the relationship between the mechanism of protein aggregation and its inhibition by heparin.

In this work, we investigate the pH-induced aggregation of three well-studied model proteins under conditions in which the native state proteins are known to form soluble complexes with heparin. The three proteins chosen for this study are bovine serum albumin (BSA), $\beta$-lactoglobulin (BLG), and Zn−insulin. BSA is a well-characterized monomeric protein that forms an equilibrium dimer.[41] Insulin, pharmaceutically formulated as the Zn hexamer, is also frequently used as a model for protein fibrilogenesis;[42] we find no difference between ambient and physiological temperature. BLG, which forms a dimer under the conditions studied, represents the most intensively studied aggregating protein because of its importance in the dairy industry,[43] particularly at elevated temperature, for which reason we use it to study the effect of heparin on thermal aggregation. Aggregation is followed by dynamic light scattering and turbidity at conditions of pH, ionic strength, and stoichiometry, compatible with both equilibrium heparin complexation and appropriate rates of aggregation. DelPhi electrostatic potential modeling facilitates interpretation of the effects of those variables. The results are organized as follows: (1) native state aggregation is reported for BSA, BLG, and Zn−insulin, and the results are discussed in terms of probable aggregation mechanisms; (2) companion studies in the presence of heparin are presented, and those results are contrasted and interpreted vis-à-vis the different mechanisms inferred in the first section; (3) a similar approach is applied for BLG under conditions of thermal denaturation with its potentially more complex set of intermediates.

## EXPERIMENTAL SECTION

**Materials.** Bovine serum albumin (BSA, 68 kDa, pI = 4.9) with total free acid content ≤1.2 mg/g was purchased from Roche Diagnostics (>95%, electrophoretically homogeneous, Indianapolis, IN). Purified bovine $\beta$-lactoglobulin (BLG, 18 kDa, pI = 5.2) was a gift from C. Schmitt (Nestle, Lausanne; >97%, batch number: JE 001-8-415). Zn−insulin (34.8 kDa, pI = 5.3) was a gift from Eli Lilly Corp. Heparin (nominal MW 14 kDa) was purchased from Sigma (Catalog No. H3393, Lot B53104). NaCl, sodium phosphate (monobasic), and standard NaOH and HCl solutions were purchased from Fisher Scientific. Milli-Q water was used in all sample preparation.

**Turbidimetric Titrations.** Solutions of BSA or BLG were prepared at the desired concentration of NaCl (5−10 mM) and pH (3−3.5 or pH 9−10, depending on the direction of pH change in subsequent pH titration) and filtered (0.22 $\mu$m Millipore). Zn−insulin solution was prepared in phosphate (10 or 30 mM) at pH 9 and filtered. Turbidimetric titration was carried out by the addition of either 0.1 N NaOH, 0.1 N HCl (for BSA and BLG), or 1 N HCl (for insulin) to a total solution volume of 10.0 mL with stirring and simultaneous monitoring of pH and transmittance. pH was measured with a Corning 240 pH meter. Transmittance of BSA solutions was measured using a Brinkmann PC 800 colorimeter equipped with a 420 nm filter and a 4 cm path length fiber optics probe; a 2 cm path length was used for BLG and Zn−insulin. After suitable warm-up, the instrument drift over this time period was as less than 0.05% (in %T), that is, introducing a relative error of less than ±0.0005%. Solutions of protein and heparin were prepared by mixing appropriate stock solutions in 1:1 v/v ratio to achieve corresponding concentrations of proteins and heparin. To test aggregation reversal, aggregated proteins were prepared by incubating at ambient conditions and the desired pH, followed by addition of 10 or 24 g/L heparin prepared at the same pH. Because the molecular stoichiometry of complexes is not yet

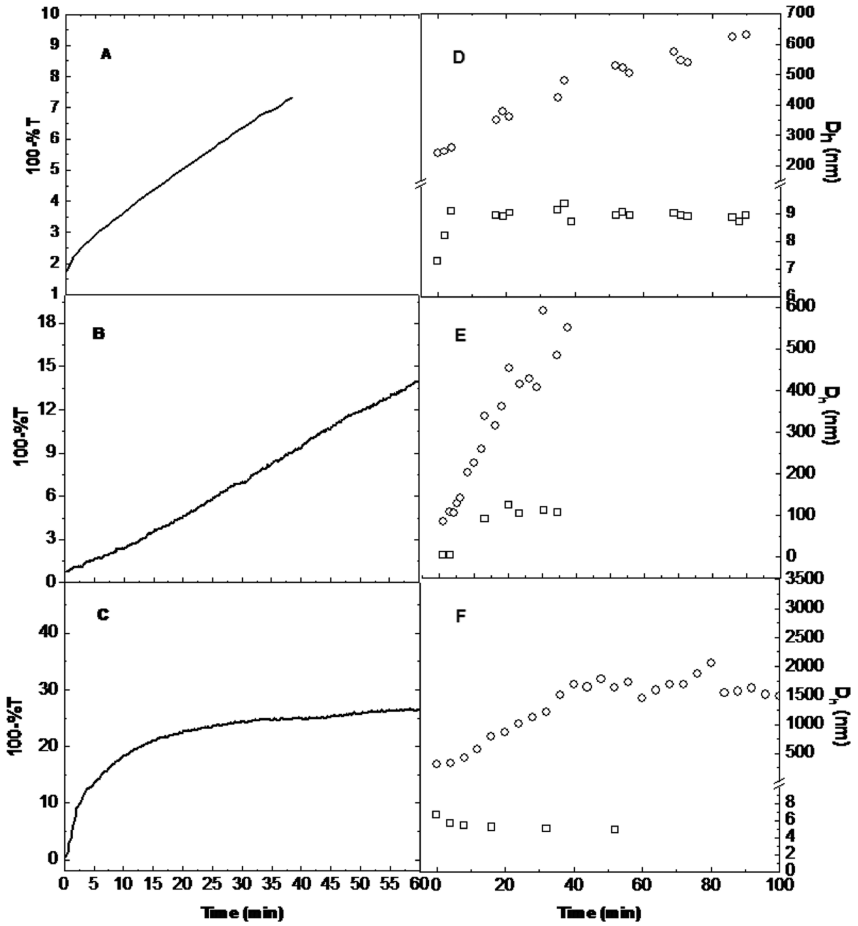


**Figure 1.** Time dependence of turbidity (left), DLS apparent size distribution (right). BSA: (A, D) pH = 5.0, $I$ = 10 mM, $C_{pro}$ = 1 g/L. BLG (B, E, data obtained from ref 54): pH = 5.2, $I$ = 4.5 mM, $C_{pro}$ = 1 g/L. Zn−insulin: (C, F) $I$ = 10 mM, pH = 5.5 (turbidity), 5.9 (DLS), $C_{pro}$ = 0.3 g/L (increased in F to 2 g/L). Symbols used to distinguish fast (□) and slow (○) modes. The first measurement (within 1 min of pH adjustment) defines zero time.

known, wt ratio is a good preliminary approach in our experiments, especially with excess heparin (molar basis).

**Dynamic Light Scattering (DLS).** DLS was carried out at 25 or 80 °C with a Malvern Zetasizer Nano ZS instrument equipped with temperature control and using a 633 nm He−Ne laser for backscattering at 173°. The measurement duration was 10 s, and 11 measurements were averaged for each analysis. The distributions of the mean apparent translational diffusion coefficients ($D_T$) were determined by fitting the DLS autocorrelation functions using nonnegative constrained least-squares (NNLS). The distribution of apparent diameters $D_h$ was obtained from the distribution of mean apparent translational diffusion coefficients ($D_T$) via

$$D_h = 2kT/(6\pi\eta D_T) \quad (1)$$

where $k$ is the Boltzmann constant and $\eta$ is the solvent viscosity which was assumed to be that of water. The protein solution was adjusted to the desired pH by NaOH and filtered into a 1 mL low volume cuvette using Whatman 0.22 $\mu$m filter. Filtration, transfer, and automated optimization steps result in a delay of 3−4 min between initial pH adjustment and the first measurement, as compared to delays of less than 20 s for turbidimetry.

**Computational Methods.** Electrostatic modeling was used to visualize the electrostatic potential around the protein as a function of pH and ionic strength. DelPhi V. 4r1.1 was used to calculate the electrostatic potential around the protein by solution of the nonlinear Poisson−Boltzmann equation.[44] Pdb 3V03 (monomeric BSA), 1BEB (dimeric BLG), and 1AI0 (hexameric Zn−insulin) were obtained from the RCSB Protein Data Bank (http://www.rcsb.org). Amino acid charges were generated using the spherical-smeared-charged model proposed by Tanford,[45] utilizing the titration curve of each protein,[46−48] as previously described.[49]

## RESULTS AND DISCUSSION

**Native Protein Aggregation Kinetics.** Heparin may interact not only with the protein itself, but also with associative protein oligomers, clusters or particles that might form in the presence of heparin. Protein structure and solution conditions (pH, ionic strength, protein concentration) influence both the kinetics and mechanism of protein aggregation, and the magnitude and form of heparin−protein complexes. We chose conditions close to the pH and ionic strength (5.3 ± 0.2, $I$ = 5−10 mM) of incubation prior to heparin addition. This corresponds to pH, $I$ conditions under which each protein forms soluble complexes with heparin and also undergoes self-aggregation in the absence of heparin. Protein concentrations were adjusted to result in levels of aggregate consistent with precision of turbidimetry and DLS.

Figure 1A−C, which shows the evolution of turbidity and diameter distributions for BSA, BLG, and Zn−insulin, indicates striking differences in kinetics and aggregation mechanisms among the three proteins. For BSA, shown in Figure 1A, the time dependence of turbidity shows the absence of a plateau. The DLS results in Figure 1D are clearly bimodal and are presented as the time dependence of the apparent hydrodynamic diameter $D_h$ for fast and slow modes, respectively. The


dx.doi.org/10.1021/bm3003539 | Biomacromolecules 2012, 13, 1642−1651

three data points within the first 10 min correspond to formation of dimer (9 nm) from monomer (7.3 nm), in accord the monomer−dimer equilibrium for BSA reported by Fullerton using osmometry.[41] but this fast mode does not subsequently change with respect to diffusivity or amplitude (Figure 2). While the increase in the apparent diameters of the

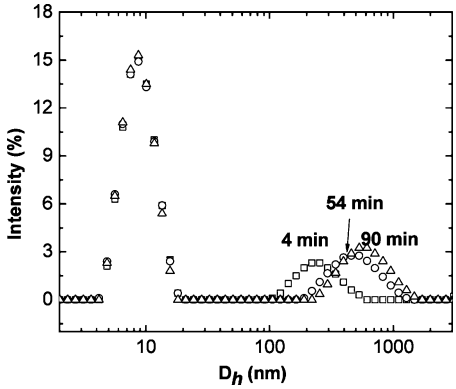


**Figure 2.** Intensity weighted diameter distributions for BSA 1 g/L, pH 5.0, $I$ = 10 mM, showing the growth of aggregates (4−90 min).

aggregate from 250 to 600 nm is accompanied by an increase in scattering intensity, the fast mode scattering is always dominant. Thus particle growth subsequent to the initial formation of 250 nm "clusters" within the first minute arises exclusively by their combination and does not involve consumption of monomer/dimer. Such cluster−cluster association is also evidenced by the absence of a turbidity plateau (Figure 1A) and by the logarithmic dependence of apparent hydrodynamic diameter on time[50,51] (Figure 3):

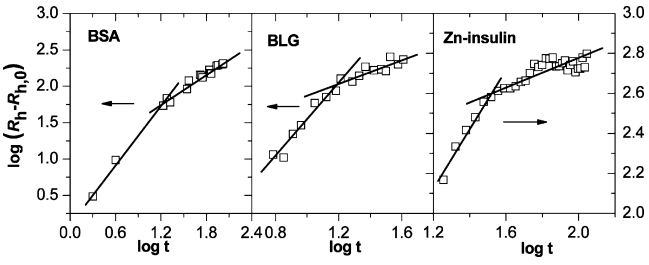


**Figure 3.** Logarithm dependence of hydrodynamic diameter on time (minutes) for BSA, BLG, and Zn−insulin. Slopes at long time regimes are 0.6 ± 0.1, 0.8 ± 0.1, and 0.4 ± 0.04, respectively. Calculated $d_f$ of three proteins at long time regimes are 1.6 ± 0.2, 1.2 ± 0.2, and 2.6 ± 0.3 respectively. Derived from data of Figure 1D−F.

$$R_h = R_{h,0} K t^{1/d_f} \quad (2)$$

where $R_h$ is the apparent hydrodynamic radius, $R_{h,0}$ is the apparent hydrodynamic radius of aggregates at $t$ = 0, $K$ is a constant, and $d_f$ is the fractal dimension. The final slope leads to a fractal dimension of $d_f$ = 1.6 ± 0.2 very close to the value of 1.8 characteristic of three-dimensional diffusion-limited aggregation of clusters (DLCA).[52,53]

Data for BLG from previously reported results[54] are shown in Figure 1B. Similar to BSA, these show no turbidity plateau, and the observed overall change in turbidity is of similar magnitude to the results for BSA. In contrast to BSA, the BLG dimer reactant is fully consumed after 5 min and the simultaneously formed 100 nm species appear to be precursors for the formation of large aggregates. The existence of such intermediate species as precursors has been clearly noted at pH 4.2 (Figure S1, Supporting Information) in which the formation of 200−500 nm intermediates is followed by their depletion, simultaneous with the appearance of 600 nm aggregates. It is noteworthy that a small reduction in pH to 4.0 appears to suppress further aggregation of species seen as intermediate at pH 4.2. The 10× increase in turbidity for BLG during the first 40 min, relative to 3× for BSA in the same time frame, could be related to the slow mode species: their size increases during first 40 min at least 3× faster than do slow mode species of BSA. In summary, intermediate species are precursors for large aggregates for BLG, whereas for BSA the aggregates are not intermediate species, but themselves undergo diffusion-limited association. The fractal dimension obtained according to eq 2 is 1.2, significantly lower than the value of 1.8 expected for DLCA.[52,53] This low value might correspond to diffusion-limited association if the distribution of proteins in the aggregate is nonuniform.

The results for Zn−insulin are shown in Figure 1C,F in which protein concentration used for turbidimetry is reduced to 0.3 g/L due to the rapidity of aggregation, but raised to 2 g/L to allow for adequate detection of the Zn−hexamer in the presence of the strong scattering from the large aggregates seen even at short time. DLS and turbidity are dramatically different from those of BSA and BLG: rapid aggregation in the first 5−10 min is followed by a plateau in both turbidity and size after about 40−50 min. The plateau also observed by DLS corresponds to aggregates much larger than those seen for BSA or BLG. The signal from the Zn−hexamer (the nonaggregated form at this pH) disappears at 50 min, which may be due in part to a shift in the distribution between hexamer and smaller multimers. The initial 200 nm aggregates formed by the relatively rapid nucleation of Zn−hexamer subsequently grow through the further addition of Zn−hexamer to these aggregates, that is, via "nucleation and growth".[55,56] Increase of the temperature to 37 °C does not appear to change the mechanism of aggregation but results in a modest increase in the apparent diameter and final turbidity (data not shown). This is consistent with other observations of Zn−insulin aggregating at pH 4−9, although aggregate size did not exceed 20 nm diameter (at $I$ = 100 mM).[57]

**Inhibition of Native State Protein Aggregation.** The ability of heparin to inhibit aggregation at some chosen pH and ionic strength arises from the competition of soluble complex formation with aggregation. Three critical pH conditions define this range when complex formation is induced by addition of acid: $pH_c$, the onset of complex formation; $pH_\varphi$, the onset of heparin−protein phase separation arising from complex charge neutralization;[28,29] and $pH^o_{agg}$, the pH at which self-aggregation is first observed. Inhibition by heparin is observed when $pH_c > pH^o_{agg} > pH_\varphi$. $pH^o_{agg}$ depends on ionic strength $I$ and protein concentration, while $pH_\varphi$ depends on $I$ and heparin/protein stoichiometry $r$. In contrast, $pH_c$ depends only on $I$ and can be observed "on the wrong side" of pI (here, $pH_c > pI$) because of protein "charge patches".[58,59] When $pH_c > pH^o_{agg}$, making inhibition possible, the pH range for aggregation inhibition is $pH^o_{agg} - pH_\varphi$. This can be expanded if $pH_\varphi$ is reduced via excess heparin (an increase in the heparin/protein ratio $r$). This reduces the number of proteins bound $n$ per heparin chain, so that the net charge of the complex $Z_T = Z_{Hp} + nZ_{pr}$ becomes more negative. This must be compensated for by lowering the


dx.doi.org/10.1021/bm3003539 | Biomacromolecules 2012, 13, 1642−1651

pH to make $Z_{pr}$ more positive. This effect is seen for all three proteins in Figure 4.

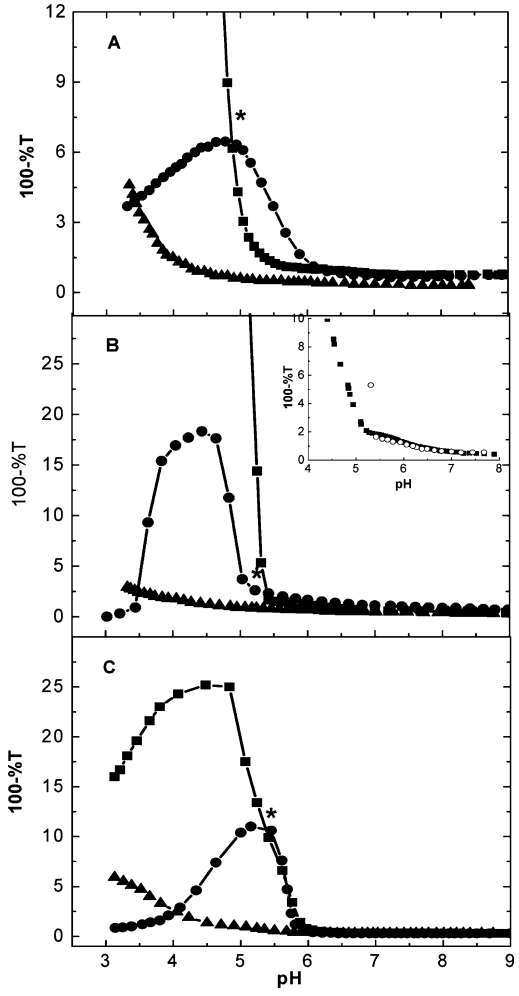


**Figure 4.** Turbidimetric titrations (addition of HCl) of 0.6 g/L (8.8 $\mu$M) BSA (A), 0.6 g/L (33 $\mu$M) BLG (B), and 0.2 g/L (34 $\mu$M) Zn–insulin (C) with heparin/protein weight ratio ($r$) of 0 (●), 0.1 (■), and 1 (▲). The corresponding molar ratios of heparin:protein are 0, 0.49, 4.9 for BSA, 0, 0.13, 1.3 for BLG, and 0, 0.25, 2.5 for Zn–insulin hexamer. Ionic strength 10 mM, except for 5 mM for BLG. Inset of B shows effects of varying titration rate for titration of BLG and heparin ($r$ = 0.1), overall titration times of 35 (■) and 12 (○) min.

Figure 4 shows how the effect of added heparin depends on protein. Upon further reduction of pH, approaching pI, complex formation leads to phase separation for BSA–heparin and BLG–heparin at $pH_\varphi$ = 5.1 and 5.2, respectively. For Zn–insulin, $pH_\varphi$ is difficult to distinguish from self-aggregation, although the causal relation between complex charge neutralization and phase separation makes $pH_\varphi$ > pI unlikely.[28] Inhibition of protein aggregation is observed most clearly for BSA around pH 5.5 where the regions of soluble complex formation ($pH_c - pH_\varphi$) and self-aggregation coexist.

All $pH_c$ values in Figure 4 are on the "wrong side of pI" (net protein charge is negative), indicating that heparin binds to a positive protein charge patch.[31] The "charge patch", representing the spatial domain in which some sequence of the heparin chain resides in its bound state, does not correspond to the protein surface but to a region of highly positive electrostatic potential,[60] best displayed in the DelPhi images of Figure 5.

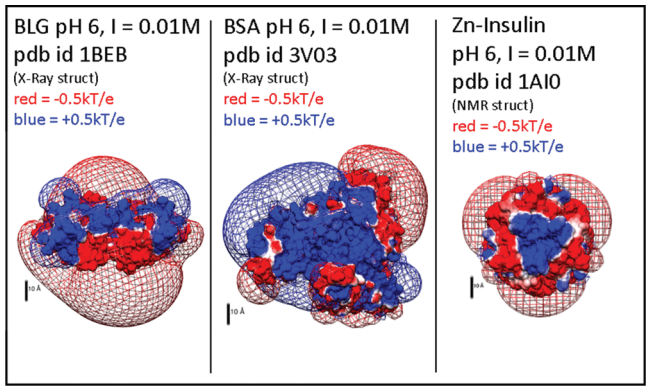


**Figure 5.** Electrostatic potential contours (−0.5 (red) and +0.5 (blue) kT/e) of BLG dimer, BSA, and Zn–insulin hexamer at pH 6, $I$ = 10 mM. The positive domain of BSA can clearly accommodate a large portion of the heparin chain (more than 5 disaccharides, containing on average 25 charges) within the +0.5 kT/e potential region. The positive domain for the BLG dimer has two nodes of high potential but they are separated by about 3 nm. The insulin (Zn) hexamer has essentially no positive patch but widely separated domains that are unlikely to accommodate more than a heparin disaccharide.

The magnitude of $pH_c$ − pI (the ability of local binding to overcome the repulsion between heparin and globally negative protein) for the three proteins is given in Table 1. These values qualitatively reflect the strength of heparin–protein interaction, i.e. its ability to lead to the formation of soluble complexes that compete with aggregation. Thus BSA with the largest Hp–protein affinity is found to show between pH 6 and 5 the largest inhibition of aggregation by heparin, even at the lowest heparin concentration. The values of $pH_c$ in Table 1 are consistent with the heparin binding constant of BSA ($1.3 \times 10^4$ at $I$ = 10, pH 6.5[49]), larger than that for BLG by a factor of 200.[61] More qualitatively, $pH_c$ for BSA is larger than that of BLG and Zn–insulin by 0.6 and 1.3 pH units, respectively, suggesting weaker binding even though Zn–insulin is the most basic protein. This order of binding is also consistent with the size at pH 6, $I$ = 10 mM of the proteins' positive domains (Figure 5).

The binding affinities described above reflect the interaction between heparin and isolated free protein. Differences noted in Figure 4 may also arise from heparin binding to other species formed during aggregation. The absence of species between free BSA and aggregates >240 nm in Figure 1D indicates a "cluster" formation step, which is inhibited in the presence of heparin by complexation of free BSA. Figure 4B and its inset show a significant increase in turbidity between $pH_c$ (which is not clearly definable in this case) and $pH_\varphi$, which is not seen for BSA. The much smaller affinity for heparin for BLG does not allow significant complexation with the BLG dimer. We therefore suggest that for BLG complexation can be *concurrent* with an early stage of the process that leads to aggregation. A similar model was also proposed by Kelly et al.,[62] who studied the binding of heparin to the unstructured 8 kDa gesolin fragment and found binding only to 40–60 nm diameter "oligomers" formed from this fragment. In the present case, the corresponding 80–100 nm BLG species, similar to the "oligomer" reported by Kelly,[62] forms a stable complex with heparin. Here we distinguish between oligomers and aggregates by viewing the former as isodesmic and therefore subject to equilibria among all species. While Kelly et al suggested that heparin serves as template for the progressive union of heparin-bound clusters, the absence of time-dependence for $pH_c$ > pH


dx.doi.org/10.1021/bm3003539 | *Biomacromolecules* 2012, 13, 1642–1651

**Table 1. Characteristic Features of pH Titrations in Figure 4**

| | pI | $pH_c$ | $pH_\varphi$ | $pH^\circ_{agg}$ | $pH_\varphi - pH_c$ | $pH_c - pI$ |
|---|---|---|---|---|---|---|
| Zn−insulin | 5.3 | 5.8 ± 0.3 | NA | 6.0 ± 0.1 | NA | 0.5 |
| BSA | 4.9 | 7.1 ± 0.1 | 5.1 ± 0.1 | 6.2 ± 0.2 | 2.0 | 2.2 |
| BLG | 5.2 | 6.5 ± 0.3 | 5.2 ± 0.1 | 6.0 ± 0.3 | 1.3 | 1.3 |

> $pH_\varphi$ (Figure 4B, inset) suggests that the increase in turbidity corresponds to an equilibrium process, that is, association of intrapolymer complexes between heparin and BLG oligomers, similar to soluble PE−protein aggregates comprising many proteins and more than one polymer chain.[63] Upon approach to pI, the net charge of intercomplexes is reduced allowing for their open-ended association and leading to a large increase in turbidity at pH 5. BSA, in contrast, forms stable <20 nm BSA−heparin intrapolymer complexes[31] (Figure 4A) favored by the abundance of BSA dimer and its high heparin affinity.[31,61] For Zn−insulin, the growth of aggregates appears to be least affected by heparin. We propose that this is a reflection of the weak heparin−Zn−insulin interaction together with rapid self-aggregation of Zn−insulin at pH 5.9 (Figure 4C). Despite weak binding at pH > pI, the presence of heparin strongly increases the turbidity at pH ≈ pI. With approach to pH 5.3, the small positive domains of Zn−insulin (the most basic of the three proteins) will expand, allowing heparin to bridge the clusters formed during self-aggregation of Zn−insulin.[55]

For all three proteins, the inhibition windows defined as $pH_c - pH^\circ_{agg}$, are considerably extended thorough increasing $r$ from 0.1 to 1; this diminishes the number of proteins bound per heparin chain and so makes the complex more negative, reducing $pH_\varphi$ to <3.5 for all proteins. Notably, Zn−insulin aggregation is strongly inhibited by this increase in heparin concentration. The weak intrinsic binding of heparin mentioned above is then compensated by its concentration, allowing it to interfere with the rapid nucleation of Zn−insulin hexamer.[55]

**Reversal of Protein Aggregates by Heparin.** Figure 6 shows the results of addition of concentrated heparin to aggregated protein solutions. To obtain similar levels of aggregation, the initial concentration of Zn−insulin was reduced 10× to 0.2 g/L. All proteins appear to be subject to reversal of aggregation by excess heparin. The results differ with respect to the time required to achieve aggregate dissolution (<1 min for BSA (Figure 6A) and BLG (Figure 6B), very slow for Zn−insulin (Figure 6C)). The terminal value of turbidity is comparable to the turbidity observed in the soluble complex region (Figure 4) for the case of BSA and Zn−insulin but significantly larger for BLG. This suggests that the complete dissolution of BSA occurs because the aggregates are sufficiently "open" (fractal dimension 1.6) to allow contact with heparin not only on the aggregate surface but also internally. Prior studies of the BSA−heparin complexes show corresponding diameters are less than 12 nm; therefore, the final products of dissolution are likely to be intrapolymer complexes rather than those involving more than one heparin chain.[31] In contrast, for BLG, the terminal turbidity is too large to arise from typical heparin−dimer soluble complexes. The addition of heparin to BLG aggregates does not recover the same state that existed when identical conditions of pH, and protein and heparin concentrations were reached by titration with HCl (Figure 4B). The process of disaggregation at pH 5.2 (pH = pI) involves initial interaction of heparin with an aggregate whose net charge is near zero. Because protein

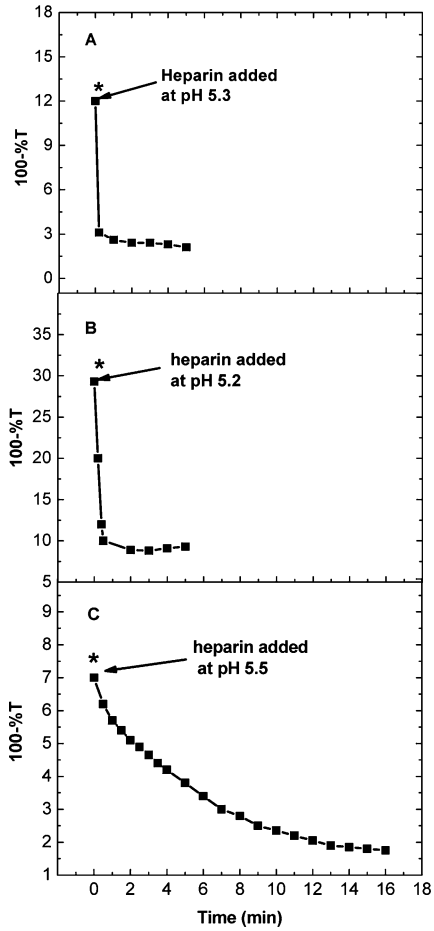


**Figure 6.** Reversal of aggregation upon addition of heparin. (A) BSA, (B) BLG, and (C) Zn−insulin were incubated for 10 min at pH 5.3 ± 0.2 to reach the desired turbidity. A total of 24 g/L of heparin was added to achieve heparin/protein ($r$) = 1. Protein concentrations $C_{pr}$ were 2 g/L with the exception of Zn−insulin ($C_{pr}$ = 0.2 g/L). The corresponding molar ratios are 4.9, 1.3, and 2.5 for BSA, BLG, and Zn−insulin hexamer, respectively. Ionic strength $I$ = 10 mM with the exception of BLG ($I$ = 5 mM). *Indicates the point at which heparin was added. The much higher turbidity for BLG before heparin addition than that in Figure 4B is because the solution was allowed to aggregate at pH 5.2 for 15 min first.

charges are labile, we propose that disproportionation can allow some surface proteins to acquire a net positive charge, bind to heparin, and be rapidly removed from the surface. This would result in the accumulation of negative charge on the aggregate, thereby reaching a terminal turbidity larger than for soluble complex but smaller than the initial aggregate.[59,64,65] This effect should be more prominent for the more negative BSA aggregates (pH − pI = 0.4). However, the more complete dissociation of aggregates of BSA versus BLG could also be explained by the stronger heparin-binding of free BSA. While the results for Zn−insulin (Figure 6C) show that heparin can reverse its aggregation, the process is very slow; nevertheless, full recovery of the low turbidity heparin−insulin intrapolymer


dx.doi.org/10.1021/bm3003539 | Biomacromolecules 2012, 13, 1642−1651

complex is seen. Static and dynamic light scattering studies with Zn−insulin aggregates showed high density (diffusivity scaling with MW only to the 0.24 power) but were also interpreted to suggest that density increases with aggregate size aggregation,[66] consistent with our observation of the highest fractal dimension for the insulin aggregate. Explanation of the slow kinetics of disaggregation rests on the presumed density of the aggregate relative to BSA or BLG (fractal dimension $d_f$ = 2.6 vs 1.6 or 1.2), a result of the aggregation mechanism. The relatively weak charge domains of the Zn−insulin hexamer at pH 5.5 (Figure 5) suggest that aggregation can be dominated by the same short-range forces responsible for crystallization.[67,68] Thus, strong interhexamer interactions and greater cohesiveness of the Zn−insulin aggregate can explain the slow dissolution with heparin.

The results presented above can be summarized as follows: The multiple ways in which heparin can affect the aggregation of a native protein depend on (1) heparin−protein affinity, (2) the competition with protein aggregation kinetics, and (3) the compactness and charge of the resultant complex. The three proteins here differ with respect to all of these effects (Scheme 1). (1) Heparin affinity, as observed by the degree to which binding occurs above pI, is greatest for BSA and least for Zn−insulin. This can be related to protein charge anisotropy, namely the influence of a protein positive domain. (2) Competition of complexation with aggregation for Zn−insulin is diminished by two effects: (a) Complexes of heparin with BSA and BLG are soluble over a wide pH range, while complexes with Zn−insulin at $r$ = 0.1 phase separate more readily, that is, at pH only slightly below the onset of complex formation; (b) The aggregation of Zn−insulin at pH near pI is more rapid than for the other proteins. (3) The slower rate of disaggregation for Zn−insulin may be related to the compactness of the aggregate $d_f$ = 2.5, possibly related to strongly ordered interactions in the aggregate.[55] For BSA the comparable "reactant" is controlled by the monomer−dimer equilibrium, and for BLG the aggregation "reactants" are oligomers. Finally, the ability of heparin to reverse protein aggregation, seen for all three proteins, depends on the susceptibility of the aggregate to permeation and dispersion by heparin, which appears to be least for the strongly cohesive Zn−insulin particles.

**Scheme 1. Proposed Mechanisms for the Effects of Heparin on Native State Aggregation**[a]

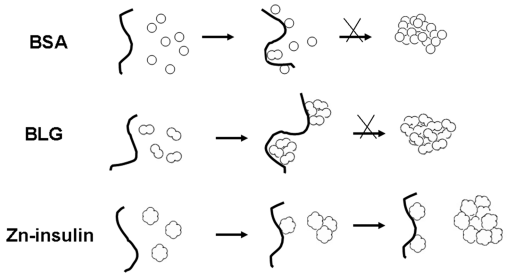


[a] $r$ = 0.1.

**Effect of Heparin on Denaturing BLG Aggregation.** If the mechanism of self-association influences heparin inhibition and reversal of aggregation, dramatic differences might be expected for unfolding versus native state aggregation. The well-studied thermally induced aggregation of BLG at 80 °C,[69−71] slightly above the midpoint of protein melting, commonly reported as $T_m$ = 73−77 °C,[72,73] at $I$ < 100 mM, was chosen for this purpose. While comparison with the pH titration results at ambient conditions would be of interest, those procedures could not be followed for technical reasons at $T \approx T_m$. Therefore, aggregation of BLG at 80 °C in the presence and absence of heparin was followed by DLS, under the same conditions of protein concentration and ionic strength used at ambient temperature. The selection of pH = 5.5 was based on observations of initial complex formation, onset of self-aggregation (Figure 4B), and proximity to the pH for aggregate reversal (Figure 6B).

The suppression of BLG aggregation at 80 °C by heparin seen in Figure 7 is evidence of the interaction of heparin with some precursor or intermediate in the aggregation process. Although there are minor discrepancies in the mechanisms of thermal BLG aggregation proposed in the literature, there is wide agreement about the initial steps in thermal aggregation, that is, that BLG loses on the order of 90% of its native structure within 12 to 15 min at $T > T_m$.[74−77] Although the nature of ultimate or intermediate species may be sensitive to conditions, it is apparent that the aggregation of denatured protein is initiated by the rate-determining dissociation of dimer to monomer,[76,78] the species considered most suscep-

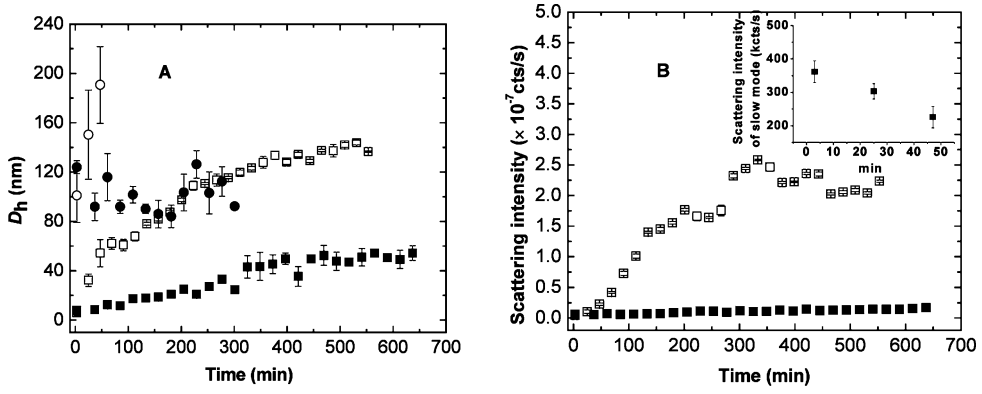


**Figure 7.** Time dependence of dynamic light scattering for 1 g/L BLG at 80 °C in 5 mM, pH 5.5 with (filled symbols) and without (open symbols) heparin. pH was rapidly adjusted from 8 to 5.5 immediately before transfer to the cell, which was then brought to 80 °C prior to the first measurement. Apparent diameters in (A): fast mode (□, ■), slow mode (○, ●); (B): corresponding total scattering intensity in the absence (□) and presence (■) of heparin. Inset of B shows scattering intensity of slow mode without heparin.

**Scheme 2. Proposed Mechanisms for the Effect of Heparin on Thermally Induced BLG Aggregation**

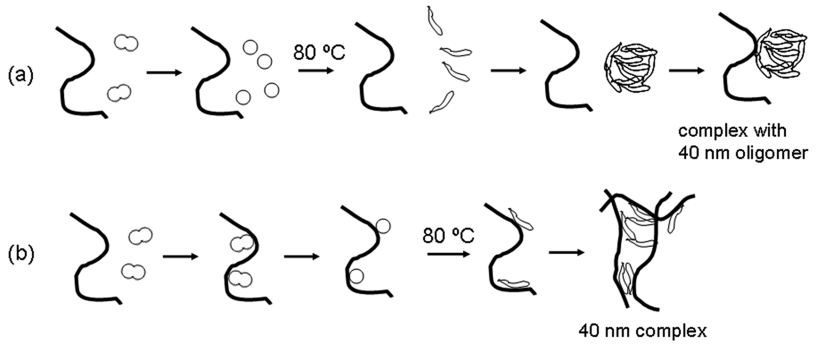


tible to rapid and irreversible unfolding above $T_m$. Conversion of dimer to monomer, in principle an equilibrium, is kinetically controlled by the slow conversion of unfolded monomer to aggregate. Here, all three processes, dissociation of dimer, unfolding of monomer, and aggregation of monomer, may in principle be influenced by the stabilizing effect of complexation with heparin, in a manner similar to the increase in $T_m$ for BLG upon complexation with dextran sulfate or $\lambda$-carrageenan.[73]

Results for heparin-free BLG in Figure 7A reveal large (100–200 nm) aggregates present during the first hour, similar in apparent diameter $D_h$ to those observed under native conditions (Figure 1E) and, therefore, possibly identical to native state aggregates (of dimers) present before heating. The slow mode diminishes in intensity and disappears in an hour, while the fast mode shows a steady increase in $D_h$ prior to reaching a plateau. Figure 7B and its inset show that the absolute amplitude of the slow mode is decreasing during the first hour, while the total intensity is increasing. The former corresponds to dissociation of the native state aggregates to free monomers, while the latter must be due to their unfolding and aggregation with an increase in $D_h$ by a factor of 8 (fast mode in 7A). After 1 h, the species arising from the unfolding and aggregation of free monomers grow from 50 to 130 nm, with a decreasing rate of growth possibly due to charge accumulation.[64,65] The presence of heparin results in three marked changes: (1) Most obvious is the dramatic reduction in total scattering intensity in Figure 7B, related to the 3-fold decrease in $D_h$ beyond 5 h in Figure 7A. (2) The stable soluble heparin–BLG complex ($D_h$ = 100 nm) diminishes in intensity (not shown) during the first 5 h, beyond which time slow and fast modes are no longer resolvable, as demonstrated by Figure S2, Supporting Information. (3) After 5 h, we observe in the presence of heparin, species that terminate at $D_h$ = 50 nm instead of ongoing aggregation of unfolded free monomers, an extension of the oligomerization during the first hour.

Because the positive domain of native BLG is most likely responsible for binding of heparin at pH > pI, the disruption of this domain upon unfolding or conversion to monomer should weaken the binding. The stronger binding of heparin to dimer shifts the monomer–dimer equilibrium and the concomitant reduction in monomer concentration impedes all further modes of aggregation. This fails to explain the increase in particle diameter up to 40 nm (terminating after 5 h) which must be accounted for by some form of association. This might involve the association of unfolded BLG to form $D_h$ < 40 nm oligomers, which then are bound by heparin; these complexes do not undergo further aggregation as indicated in Scheme 2a. Alternatively, heparin initially (at the point of heating) binds native BLG, which is predominantly dimer with some aggregate with less than 2 min of incubation; the heparin–dimer complex is also favored by the positive domain unique to the native dimer (Figure 5). This heparin-bound BLG dimer unfolds in the complexed state, and these intrapolymer complexes are then subject to association through intercomplex interactions of exposed hydrophobic BLG regions (Scheme 2b). While the native dimer may bind heparin with greater affinity, anionic polyelectrolytes can bind also unfolded proteins even at pH > pI.[30] The principal difference between these two sequences of binding/unfolding events is coulomb blocking[64,65] (in the second scenario) of the association of negatively charged heparin–oligomer or heparin–aggregate species, limiting their size to $D_h$ = 40 nm. These species cannot be formed by simply adding heparin to the 120 nm BLG aggregates. Such denatured aggregates may lack the necessary flexibility and presentation of positive charge (possibly characteristic of smaller oligomers) to allow for heparin binding to occur at any time scale and thus are irreversible.

## CONCLUSIONS

The multiple ways that heparin influences native protein aggregation depends on three factors: (1) protein–heparin binding affinity, which is a function of pH and ionic strength, and protein charge anisotropy; (2) the nature of the heparin–protein complexes so formed; and (3) the stage of the aggregation process that is directly affected by complex formation. All three of these factors influence the competition between equilibrium complex formation and kinetic aggregation. While the formation of soluble complexes can inhibit or suppress protein aggregation at certain conditions of pH, ionic strength, and stoichiometry for all the protein studied, differences in protein structure and aggregation mechanisms lead to different heparin effects. The dramatically different aggregation mechanism for a thermally unfolded protein requires a more complex interpretation of the observed heparin suppression. In this case, aggregation could not be reversed by heparin, in contrast to more "open" or loosely structured aggregates that could be dissociated to various extents.

## ASSOCIATED CONTENT

### Supporting Information

DLS results on native BLG aggregation at pH 4.0 and 4.2. DLS correlation functions of Zn–insulin at 9 and 65 min and denaturing BLG aggregation at 200 and 330 min. This material is available free of charge via the Internet at http://pubs.acs.org.

## AUTHOR INFORMATION


### Corresponding Author

*E-mail: dubin@chem.umass.edu.


### Notes

The authors declare no competing financial interest.

## ACKNOWLEDGMENTS

Support from NSF (Grant CBET-0966923) is acknowledged. We thank Eli Lilly and Co. for the gift of Zn−insulin and Dr. Christophe Schmitt (Nestle, Lausanne, Switzerland) for the BLG samples. Helpful discussions with B. Kurganov are acknowledged.

## REFERENCES


(1) Pullara, F.; Emanuele, A.; Palma-Vittorelli, M. B.; Palma, M. U. *Biophys. J.* **2007**, *93*, 3271.
(2) Cromwell, M. E.; Hilario, E.; Jacobson, F. *AAPS J.* **2006**, *8*, E572.
(3) Rousseau, F.; Schymkowitz, J.; Serrano, L. *Curr. Opin. Struct. Biol.* **2006**, *16*, 118.
(4) Bucciantini, M.; Giannoni, E.; Chiti, F.; Baroni, F.; Formigli, L.; Zurdo, J.; Taddei, N.; Ramponi, G.; Dobson, C. M.; Stefani, M. *Nature* **2002**, *416*, 507.
(5) Bucciantini, M.; Calloni, G.; Chiti, F.; Formigli, L.; Nosi, D.; Dobson, C. M.; Stefani, M. *J. Biol. Chem.* **2004**, *279*, 31374.
(6) Kayed, R.; Head, E.; Thompson, J. L.; McIntire, T. M.; Milton, S. C.; Cotman, C. W.; Glabe, C. G. *Science* **2003**, *300*, 486.
(7) O'Nuallain, B.; Wetzel, R. *Proc. Natl. Acad. Sci. U.S.A.* **2002**, *99*, 1485.
(8) Quist, A.; Doudevski, I.; Lin, H.; Azimova, R.; Ng, D.; Frangione, B.; Kagan, B.; Ghiso, J.; Lal, R. *Proc. Natl. Acad. Sci. U.S.A.* **2005**, *102*, 10427.
(9) Giger, K.; Vanam, R. P.; Seyrek, E.; Dubin, P. L. *Biomacromolecules* **2008**, *9*, 2338.
(10) Chen, B.-l.; Arakawa, T.; Morris, C. F.; Kenney, W. C.; Wells, C. M.; Pitt, C. G. *Pharm. Res.* **1994**, *11*, 1581.
(11) Meng, F.-G.; Park, Y.-D.; Zhou, H.-M. *Int. J. Biochem. Cell Biol.* **2001**, *33*, 701.
(12) Zhu, H. Y., J.; Kindy, M. S. *Mol. Med.* **2001**, *7*, 517.
(13) Tiedemann, K.; Bätge, B.; Müller, P. K.; Reinhardt, D. P. *J. Biol. Chem.* **2001**, *276*, 36035.
(14) Wallace, B. *J. Neurosci.* **1990**, *10*, 3576.
(15) Hamada, H. A., T; Shiraki, K *Curr. Pharm. Biotechnol.* **2009**, *10*, 400.
(16) Takase, K. *FEBS Lett.* **1998**, *441*, 271.
(17) Yu, S.; Yin, S.; Pham, N.; Wong, P.; Kang, S.-C.; Petersen, R. B.; Li, C.; Sy, M.-S. *FEBS* **2008**, *275*, 5564.
(18) Lyon, A. W.; Narindrasorasak, S.; Young, I. D.; Anastassiades, T.; C., J. R.; McCarthy, K. J.; Kisilevsky, R. *Lab Invest.* **1991**, *64*, 785.
(19) Kisilevsky, R. *J. Struct. Biol.* **2000**, *130*, 99.
(20) McLaurin, J.; Yang, D. S.; Yip, C. M.; Fraser, P. E. *J. Struct. Biol.* **2000**, *130*, 259.
(21) Cohlberg, J. A.; Li, J.; Uversky, V. N.; Fink, A. L. *Biochemistry* **2002**, *41*, 1502.
(22) Relini, A.; De Stefano, S.; Torrassa, S.; Cavalleri, O.; Rolandi, R.; Gliozzi, A.; Giorgetti, S.; Raimondi, S.; Marchese, L.; Verga, L.; Rossi, A.; Stoppini, M.; Bellotti, V. *J. Biol. Chem.* **2008**, *283*, 4912.
(23) Shalova, I. N.; Naletova, I. N.; Saso, L.; Muronetz, V. I.; Izumrudov, V. A. *Macromol. Biosci.* **2007**, *7*, 929.
(24) Shalova, I. N.; Asryants, R. A.; Sholukh, M. V.; Saso, L.; Kurganov, B. I.; Muronetz, V. I.; Izumrudov, V. A. *Macromol. Biosci.* **2005**, *5*, 1184.
(25) Stogov, S.; Izumrudov, V.; Muronetz, V. *Biochemistry (Moscow)* **2010**, *75*, 437.
(26) Stogov, S.; Muronetz, V.; Izumrudov, V. *Dokl. Biochem. Biophys.* **2009**, *427*, 187.
(27) Fedunová, D.; Antalík, M. *Biotechnol. Bioeng.* **2006**, *93*, 485.
(28) Cooper, C. L.; Dubin, P. L.; Kayitmazer, A. B.; Turksen, S. *Curr. Opin. Colloid Interface Sci.* **2005**, *10*, 52.
(29) Mattison, K. W.; Brittain, I. J.; Dubin, P. L. *Biotechnol. Prog.* **1995**, *11*, 632.
(30) Vardhanabhuti, B.; Allen Foegeding, E. *Food Hydrocolloid* **2008**, *22*, 752.
(31) Seyrek, E.; Dubin, P. L.; Tribet, C.; Gamble, E. A. *Biomacromolecules* **2003**, *4*, 273.
(32) Wang, W. *Int. J. Pharm.* **2005**, *289*, 1.
(33) Uversky, V. N.; Fink, A. L.; Khurana, R.; Karnoup, A. S.; Segel, D. J.; Doniach, S. *Protein Sci.* **1999**, *8*, 161.
(34) Dong, A.; Prestrelski, S. J.; Allison, S. D.; Carpenter, J. F. *J. Pharm. Sci.* **1995**, *84*, 415.
(35) Dill, K. A. *Biochemistry* **1990**, *29*, 7133.
(36) Ju, Z. Y.; Kilara, A. *J. Agric. Food Chem.* **1998**, *46*, 1830.
(37) Sluzky, V.; Tamada, J. A.; Klibanov, A. M.; Langer, R. *Proc. Natl. Acad. Sci. U.S.A.* **1991**, *88*, 9377.
(38) De Young, L. R.; Fink, A. L.; Dill, K. A. *Acc. Chem. Res.* **1993**, *26*, 614.
(39) Khanova, H. A.; Markossian, K. A.; Kurganov, B. I.; Samoilov, A. M.; Kleimenov, S. Y.; Levitsky, D. I.; Yudin, I. K.; Timofeeva, A. C.; Muranov, K. O.; Ostrovsky, M. A. *Biochemistry* **2005**, *44*, 15480.
(40) Speed, M. A.; King, J.; Wang, D. I. C. *Biotechnol. Bioeng.* **1997**, *54*, 333.
(41) Fullertona, G. D.; Kanala, K. M.; Cameron, I. L. *Cell Biol. Int.* **2006**, *30*, 86.
(42) Nayak, A.; Sorci, M.; Krueger, S.; Belfort, G. *Proteins: Struct., Funct., Bioinf.* **2009**, *74*, 556.
(43) Lan, X. Y.; Wang, J. Q.; Bu, D. P.; Shen, J. S.; Zheng, N.; Sun, P. *J. Food. Sci.* **2010**, *75*, C653.
(44) Nicholls, A.; Honig, B. *J. Comput. Chem.* **1991**, *12*, 435.
(45) Tanford, C.; Kirkwood, J. G. *J. Am. Chem. Soc.* **1957**, *79*, 5333.
(46) Tanford, C.; Swanson, S. A.; Shore, W. S. *J. Am. Chem. Soc.* **1955**, *77*, 6414.
(47) Nozaki, Y.; Bunville, L. G.; Tanford, C. *J. Am. Chem. Soc.* **1959**, *81*, 5523.
(48) Tanford, C.; Epstein, J. *J. Am. Chem. Soc.* **1954**, *76*, 2170.
(49) Hattori, T.; Kimura, K.; Seyrek, E.; Dubin, P. L. *Anal. Biochem.* **2001**, *295*, 158.
(50) Weitz, D. A.; Huang, J. S.; Lin, M. Y.; Sung, J. *Phys. Rev. Lett.* **1984**, *53*, 1657.
(51) Chebotareva, N. A.; Meremyanin, A. V.; Makeeva, V. F.; Livanova, N. B.; Kurganov, B. I. *Biophys. Chem.* **2008**, *133*, 45.
(52) Meakin, P. *J. Sol-Gel Sci. Technol.* **1999**, *15*, 97.
(53) Weitz, D. A.; Oliveria, M. *Phys. Rev. Lett.* **1984**, *52*, 1433.
(54) Majhi, P. R.; Ganta, R. R.; Vanam, R. P.; Seyrek, E.; Giger, K.; Dubin, P. L. *Langmuir* **2006**, *22*, 9150.
(55) Xu, Y.; Yan, Y.; Seeman, D.; Sun, L.; Dubin, P. L. *Langmuir* **2011**, *28*, 579.
(56) Wang, K.; Kurganov, B. I. *Biophys. Chem.* **2003**, *106*, 97.
(57) Bohidar, H. B. *Biopolymers* **1998**, *45*, 1.
(58) Xu, Y.; Mazzawi, M.; Chen, K.; Sun, L.; Dubin, P. L. *Biomacromolecules* **2011**, *12*, 1512.
(59) Chen, K.; Xu, Y.; Rana, S.; Miranda, O. R.; Dubin, P. L.; Rotello, V. M.; Sun, L.; Guo, X. *Biomacromolecules* **2011**, *12*, 2552.
(60) Grymonpré, K. R.; Staggemeier, B. A.; Dubin, P. L.; Mattison, K. W. *Biomacromolecules* **2001**, *2*, 422.
(61) Hattori, T.; Kimura, K.; Seyrek, E.; Dubin, P. L. *Anal. Sci. (Japan)* **2001**, *17*, 93.
(62) Bourgault, S.; Solomon, J. P.; Reixach, N. l.; Kelly, J. W. *Biochemistry* **2010**, *50*, 1001.
(63) Xia, J.; Dubin, P. L.; Kim, Y.; Muhoberac, B. B.; Klimkowski, V. J. *J. Phys. Chem.* **1993**, *97*, 4528.
(64) Stradner, A.; Sedgwick, H.; Cardinaux, F.; Poon, W. C. K.; Egelhaaf, S. U.; Schurtenberger, P. *Nature* **2004**, *432*, 492.
(65) Kizilay, E.; Kayitmazer, A. B.; Dubin, P. L. *Adv. Colloid Interface Sci.* **2011**, *167*, 24.
(66) Bohidar, H. B.; Geissler, E. *Biopolymers* **1984**, *23*, 2407.

(67) Yip, C. M.; Brader, M. L.; DeFelippis, M. R.; Ward, M. D. *Biophys. J.* **1998**, *74*, 2199.
(68) Turkenburg-van Diepen, M. *Ph.D. Thesis*, University of York, U.K., 1996.
(69) Vetri, V.; Militello, V. *Biophys. Chem.* **2005**, *113*, 83.
(70) Schokker, E. P.; Singh, H.; Pinder, D. N.; Creamer, L. K. *Int. Dairy J.* **2000**, *10*, 233.
(71) Donald, A. M. *Soft Matter* **2008**, *4*, 1147.
(72) Haug, I. J.; Skar, H. M.; Vegarud, G. E.; Langsrud, T.; Draget, K. I. *Food Hydrocolloid* **2009**, *23*, 2287.
(73) Zhang, G.; Foegeding, E. A.; Hardin, C. C. *J. Agric. Food Chem.* **2004**, *52*, 3975.
(74) Zúñiga, R. N.; Tolkach, A.; Kulozik, U.; Aguilera, J. M. *J. Food Sci.* **2010**, *75*, E261.
(75) Law, A. J. R.; Leaver, J. *J. Agric. Food Chem.* **2000**, *48*, 672.
(76) Iametti, S.; De Gregori, B.; Vecchio, G.; Bonomi, F. *Eur. J. Biochem.* **1996**, *237*, 106.
(77) Sava, N.; Van der Plancken, I.; Claeys, W.; Hendrickx, M. *J. Dairy Sci.* **2005**, *88*, 1646.
(78) Qi, X. L.; Holt, C.; McNulty, D.; Clarke, D. T.; Brownlow, S.; Jones, G. R. *Biochem. J.* **1997**, *324*, 341.